

Supplementary Information

Donor-acceptor structure of coordination polymer with long-lived room temperature phosphorescence and angle-dependent polarized emission

Wen-Jing Qin,^{a,b} Ji-Rui Zhang,^a Xu-Ke Tian,^{a,b} Xiao-Gang Yang,^{b*} and Yu-Ming Guo^{a*}

^a College of Chemistry and Chemical Engineering, Henan Normal University, Xinxiang, 453007, P. R. China.

^b College of Chemistry and Chemical Engineering, Luoyang Normal University, Henan Province Function-Oriented Porous Materials Key Laboratory, Luoyang 471934, P. R. China.

*** Corresponding Author**

Tel.: 86-379-68618328, Fax: 86-20-68618320. E-mail: yxg2233@126.com

A. Experimental Section.

1. Materials and general procedures.

All reagents were of analytical grade and obtained from commercial sources without further purification. Powder X-ray diffraction analyses (PXRD) patterns were collected on a Bruker D8-ADVANCE X-ray diffractometer with Cu K α radiation ($\lambda = 1.5418 \text{ \AA}$). Measurements were made in a 2θ range of $5\text{--}50^\circ$ at room temperature with a step of 0.02° (2θ) and a counting time of 0.2 s/step . The operating power was 40 KV, 40 mA. The C, H, N analyses were carried out using a Perkin–Elmer Elementarvario elemental analysis instrument. Room temperature photoluminescence (PL) spectra and time-resolved lifetime were conducted on an Edinburgh FLS1000 fluorescence spectrometer. Thermo gravimetric analysis (TGA) experiments were carried out using SII EXStar6000 TG/DTA6300 thermal analyzer from room temperature to 800°C under a nitrogen atmosphere at a heating rate of $10^\circ\text{C min}^{-1}$. The fluorescence spectra were measured by a continuous radiation of xenon arc lamp (Xe900). The fluorescence decay curves were measured by a nanosecond flash-lamp (nF900). While the phosphorescence spectra and phosphorescence decay curves were tested by a pulsing radiation of microsecond flash lamp with time-resolved single photon counting–multi-channel scaling mode. Polarized luminescent (fluorescence and phosphorescence) spectra were measured on Edinburgh FLS1000 fluorescence spectrometer by setting a polarizer in front of the detector. The phosphorescence quantum yields at room temperature were tested using an integrating sphere (F-M101, Edinburgh) accessory in FLS1000 fluorescence spectrometer. For the detection of angle-dependent polarized fluorescence and phosphorescence spectra, the sample of title complex was irradiated by 330 nm xenon arc lamp and 380 nm microsecond flash lamp, respectively. The polarization of the light signal can be obtained by setting a polarizer in front of the detector and rotating the polarizer at different

polarization angle. Optoelectronic measurements were performed with a CHI 660E electrochemical workstation (CH Instruments, Chenhua Co., Shanghai, China) by using **1** modified indium tin oxide (ITO) as the working electrode (working area 1.0 cm²), Ag/AgCl as a reference electrode, platinum wire electrode as a counter electrode. All electrochemical tests were performed at room temperature in 0.5 M Na₂SO₄ solution. The cyclic voltammogram curve was measured in the range of -0.6 to 0.6 V by a scan rate of 50 mV/s. The electrochemical impedance spectroscopy (EIS) measurements were recorded at the potential of -0.5 V potential in the frequency range of 100 kHz to 100 mHz. The system was conducted in a quartz glass reactor about 50 cm³, and irradiated by a 300W Xe lamp. Transient photocurrent responses with the on-off cycle's illumination and constant potential electrolysis curves with bias potential of -0.5 V were tested in three-electrode system at ambient pressure and room temperature.

2. Syntheses of [Cd(EtOIPA)(phen)]·0.5(H₂O) (**1**)

A mixture of Cd(CH₃COO)₂·2H₂O (1 mmol, 266 mg), 5-ethoxyisophthalic acid (0.5 mmol, 105 mg), 1,10-phenanthroline (0.5 mmol, 90 mg), and 8 mL of DMF was stirred for 10 min. The mixture was then transferred and sealed into a Teflon reactor (23 ml), and heated at 120 °C for 48 h, and then cooled to room temperature naturally. The colorless block crystals of **1** were obtained. Anal. Calc. (%) for C₂₂H₁₈CdN₂O_{5.5}: C 51.72, H 3.55, N 5.48; found (%): C 51.03, H 3.11, N 5.79.

3. X-ray crystal structure

Single-crystal X-ray diffraction data for **1** was collected at room temperature (293K) on an Oxford Diffraction SuperNova area-detector diffractometer using mirror optics monochromated Mo K α radiation ($\lambda = 0.71073 \text{ \AA}$). CrysAlisPro¹ was used for the data collection, data reduction and empirical absorption correction. The crystal structure were solved by direct methods, using

SHELXS-2014 and least-squares refined with SHELXL-2014 using anisotropic thermal displacement parameters for all non-hydrogen atoms.² The crystallographic data for **1** are listed in Table S1 and 2. The CIF file of **1** (CCDC No. 2063993) can be downloaded free of charge via <http://www.ccdc.cam.ac.uk/conts/retrieving.html>.

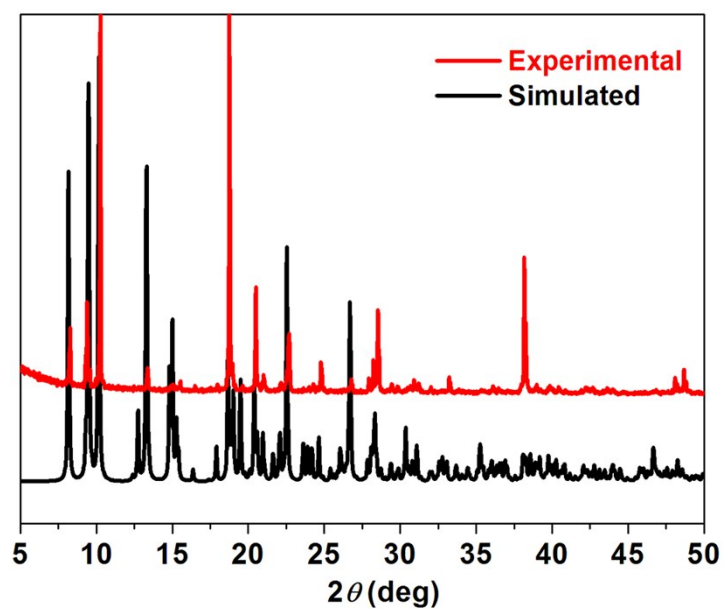
4. Preparation of working electrode

The ITO ($1 \times 4 \text{ cm}^2$) substrate was washed by ethanol, and water under ultrasonic processing for about 30 min then dried in natural environment. The complex powders (10 mg) were added into 1 mL anhydrous ethanol and ultrasonicated for 30 min to form suspension liquid. The working electrodes were prepared by dropping the above suspension (0.2 mL) onto the surface of the pre-treated ITO by controlling the coating area about 1 cm^2 , and allowing it to dry at room temperature.

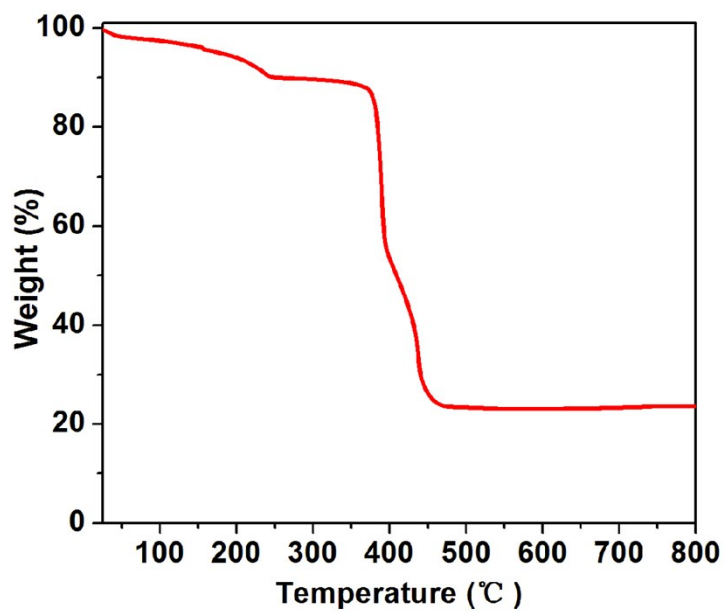
5. Theoretical calculations.

The density functional theory (DFT) calculations were performed by Material Studio software package³ Dmol3 module,⁴ based on the crystallographic information file (cif) of the title complex. Perdew-Wang (PW91)⁵ generalized gradient approximation (GGA) method was used for the full optimization of initial configuration. The self-consistent field (SCF) converged criterion was within 1.0×10^{-5} hartree atom⁻¹ and the converging criterion of the structure optimization was 1.0×10^{-3} hartree bohr⁻¹.

B. Supporting Figures



(a)



(b)

Figure S1. (a) Powder X-ray diffraction patterns (PXRD) of the simulated (black) and as-synthesized (red) title complex **1**. (b) Thermo gravimetric curve of **1**.

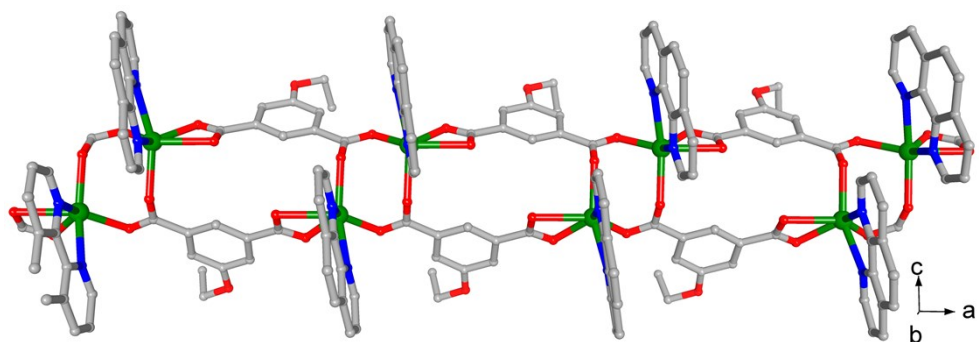


Figure S2. View of 1D double strand chain of **1** running along *a* direction.

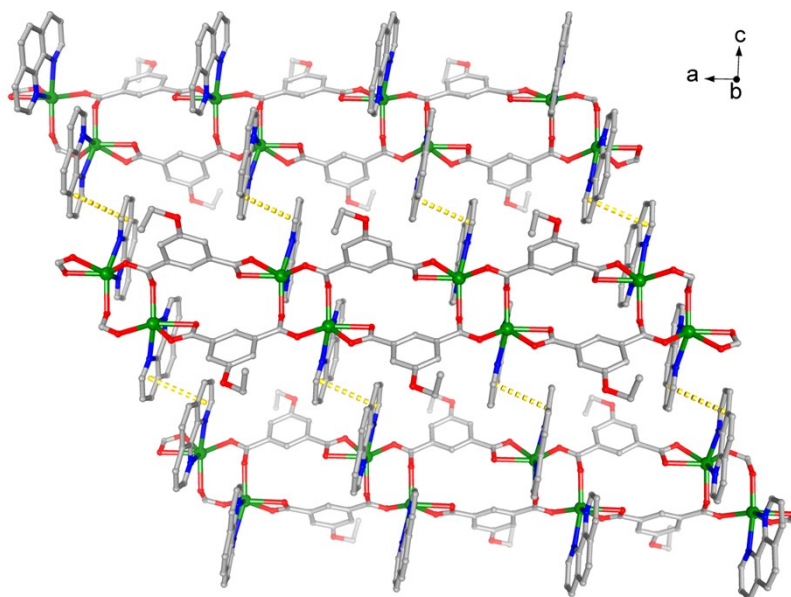


Figure S3. View of the 2D network of **1** along *ac* plane extended by $\pi \cdots \pi$ stacking between phen ligands of adjacent chains.

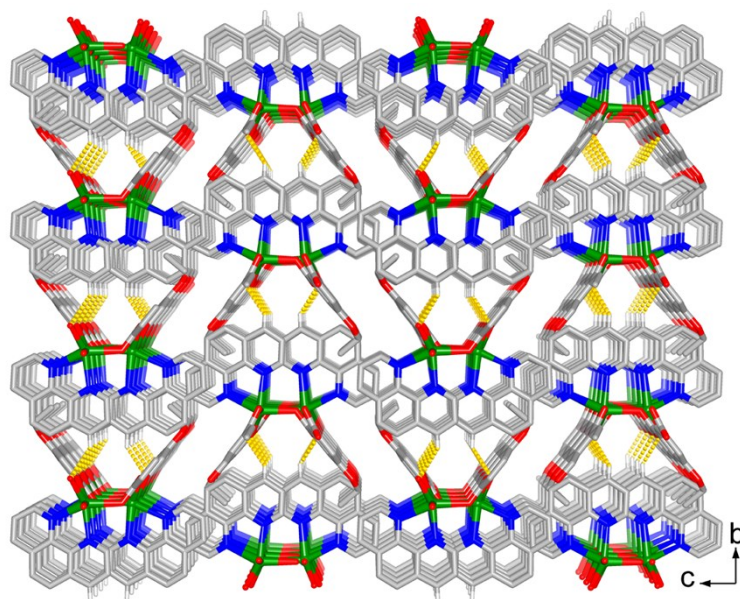


Figure S4. View of the 3D structure of **1** consists C-H...O and C-H... π interactions between 2D layers.

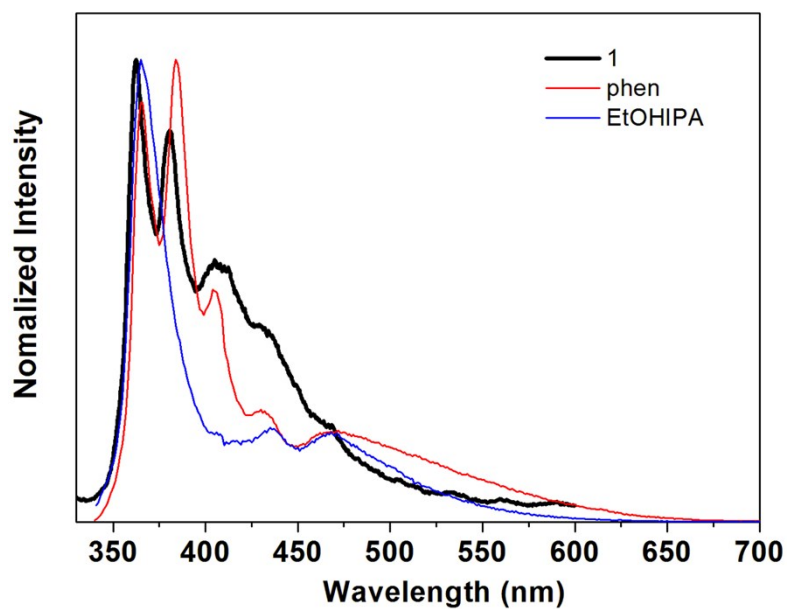


Figure S5. Normalized fluorescence spectra of complex **1**, phen and EtOIPA.

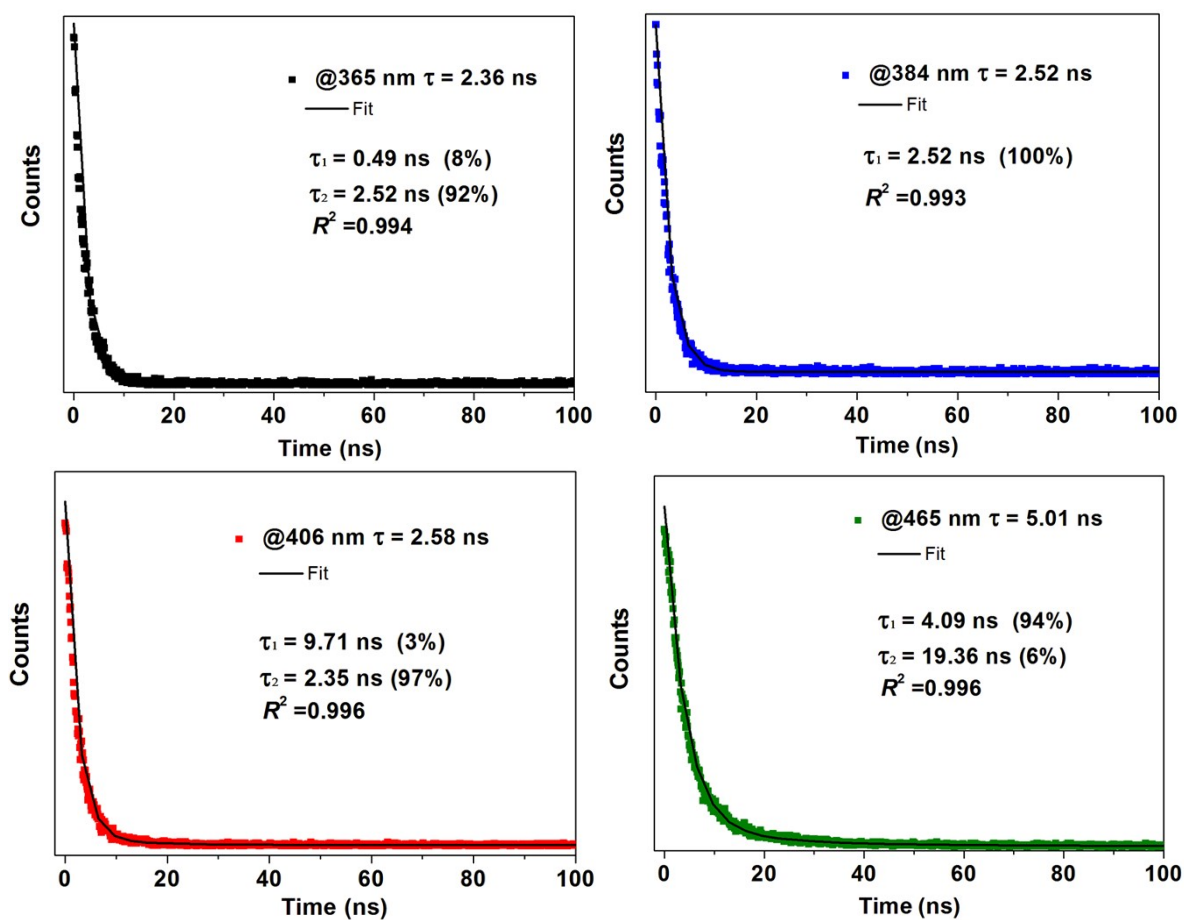


Figure S6. Fluorescence decay curves of **1** measured at room temperature.

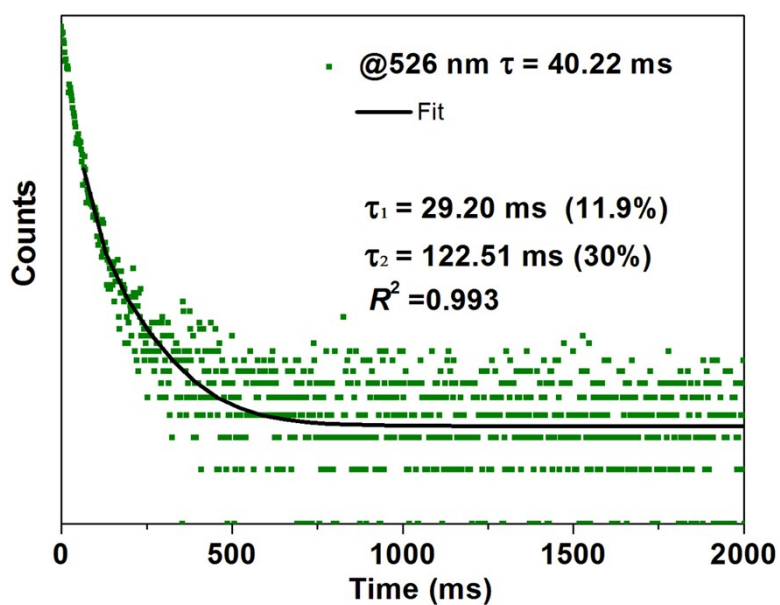


Figure S7. Phosphorescence decay curve of **1** measured at room temperature.

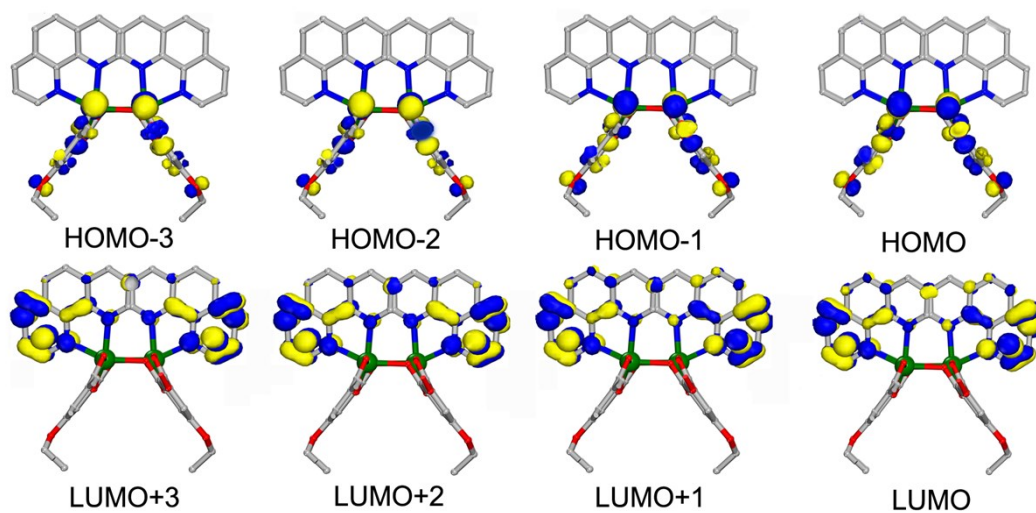


Figure S8. View of HOMOs and LUMOs for the DFT optimized structure of **1**.

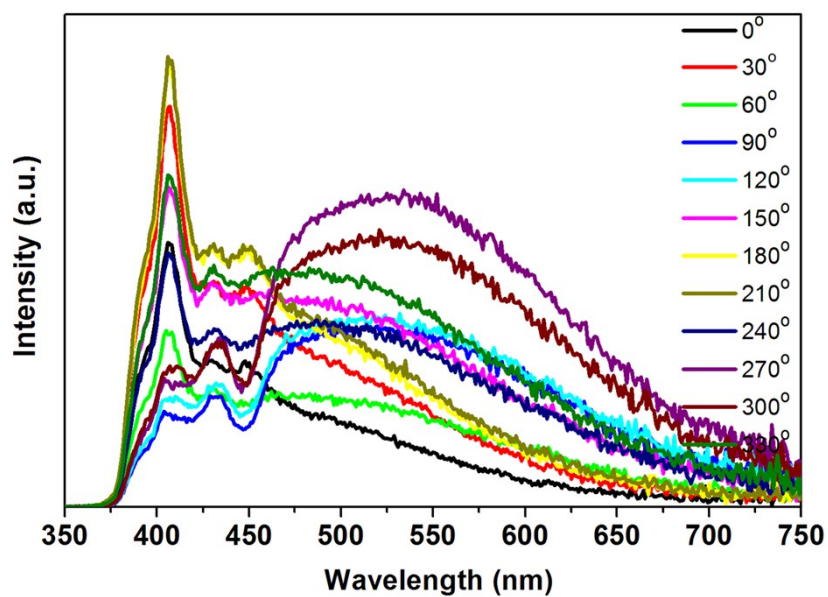


Figure S9. Angle-dependent polarized fluorescence emission of **1**.

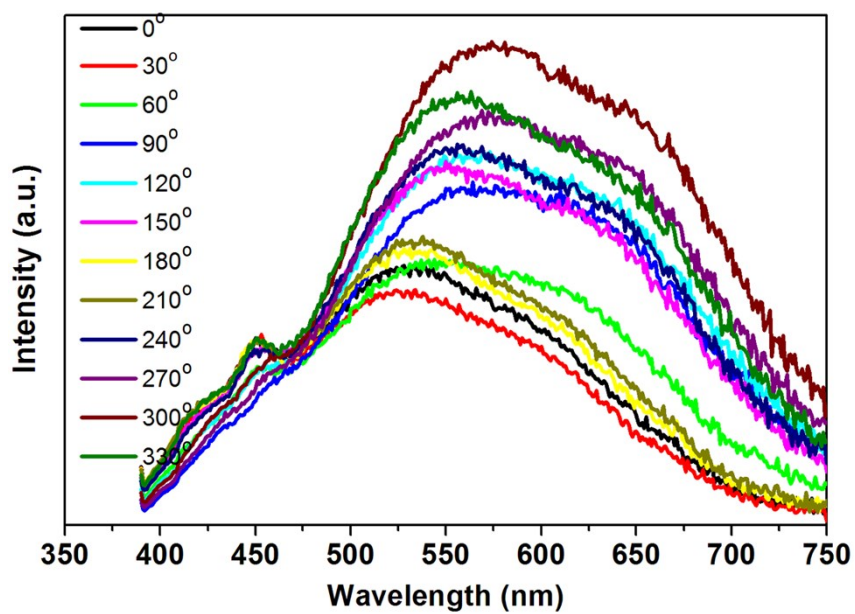


Figure S10. Angle-dependent polarized phosphorescence emission of **1**.

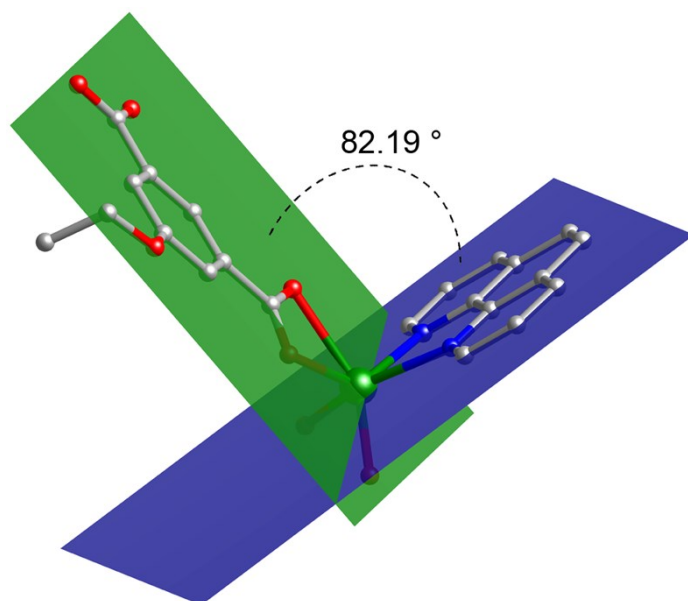


Figure S11. The dihedral angle between EtOIPA and phen ligands in **1**.

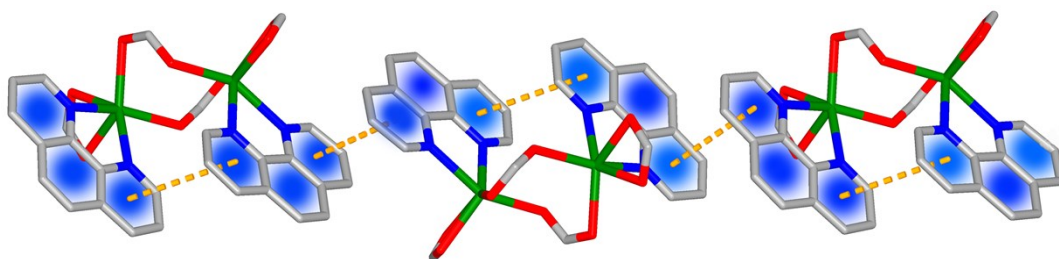


Figure S12. View of the continuous $\pi \cdots \pi$ stacking between phen ligands of adjacent chains.

C. Supporting Table

Table S1. Crystallographic data for **1**.

Samples	1
Empirical formula	C ₂₂ H ₁₈ CdN ₂ O _{5.5}
Formula weight	510.78
CCDC	2063993
Temperature/K	283
Crystal system	monoclinic
Space group	<i>P2/n</i>
<i>a</i> /Å	10.1841(3)
<i>b</i> /Å	9.5035(4)
<i>c</i> /Å	21.6676(11)
α /°	90
β /°	91.787(4)
γ /°	90
<i>V</i> /Å ³	2096.07(15)
<i>Z</i>	4
<i>D</i> (g cm ⁻³)	1.619
μ (mm ⁻¹)	1.081
<i>R</i> _{int}	0.0354
Goof	1.063
<i>R</i> ₁ (<i>I</i> > 2σ(<i>I</i>)) ^a	0.0601
<i>wR</i> ₂ (<i>I</i> > 2σ(<i>I</i>)) ^b	0.1801

$$^a R_1 = \Sigma ||F_o| - |F_c|| / \Sigma |F_o|, \quad ^b wR_2 = [\Sigma w(F_o^2 - F_c^2)^2 / \Sigma w(F_o^2)^2]^{1/2}$$

Table S2. Partial bond length and bond angle of **1**.

Atoms	Length/Å	Atoms	Length/Å
Cd1–O3#1	2.301(5)	Cd1–O4#1	2.326(6)
Cd1–O1#2	2.290(5)	Cd1–N1	2.367(6)
Cd1–O2	2.290(5)	Cd1–N2	2.341(6)
Atoms	Angle/°	Atoms	Angle/°
O1#2–Cd1–O3#1	136.30(19)	O1#2–Cd1–O4#1	82.77(19)
O1#2–Cd1–N1	85.7(2)	O12–Cd1–N2	135.24(19)
O2–Cd1–O3#1	92.0(2)	O2–Cd1–O1#2	102.9(2)
O2–Cd1–O4#1	112.5(2)	O2–Cd1–N1	152.5(2)
O2–Cd1–N2	85.2(2)	O4#1–Cd1–O3#1	53.7(2)
O41–Cd1–N1	94.3(2)	O4#1–Cd1–N2	135.0(2)
N1–Cd1–O3#1	99.7(2)	N2–Cd1–O3#1	86.2(2)

Symmetry codes: #1: 1/2-x, y, 3/2-z; #2: 3/2-x, y, 3/2-z.

D. Supporting References

1. CrysAlisPro, Rigaku Oxford Diffraction, Version 1.171.39.6a.
2. G. M. Sheldrick, *Acta Crystallogr. Sect. A* 2008, **64**, 112.
3. (a) B. Delley, *J. Chem. Phys.* 1990, **92**, 508; (b) B. Delley, *J. Chem. Phys.* 2000, **113**, 7756.
4. Dmol3 Module, MS Modeling, Version 2.2; Accelrys Inc.: San, Diego, 2003.
5. J. P. Perdew, J. A. Chevary, S. H. Vosko, K. A. Jackson, M. R. Pederson, D. J. Singh and C. Fiolhais, *Phys. Rev. B* 1992, **46**, 6671.